JOURNAL OF CATALYSIS 83, 257–266 (1983)

Carbon and Carbon Monoxide Hydrogenation on Nickel: Support Effects

SIBEL Z. OZDOGAN, PAUL D. GOCHIS, AND JOHN L. FALCONER[1]

Department of Chemical Engineering, University of Colorado, Box 424, Boulder, Colorado 80309

Received October 15, 1982; revised April 14, 1983

Hydrogenation of carbon, deposited on nickel catalysts by CO disproportionation, was investigated by temperature-programmed surface reaction (TPSR) for four oxide supports, Al_2O_3, SiO_2, TiO_2, and $SiO_2 \cdot Al_2O_3$. The rate of carbon monoxide hydrogenation was measured by temperature-programmed reaction (TPR) for comparison. The rate of carbon hydrogenation to methane was found to be independent of the support and an average activation energy of 42 kJ/mol was estimated. In contrast, the rate of carbon monoxide hydrogenation was very sensitive to the catalyst support. Nickel supported on TiO_2 exhibited the highest specific activity, and two distinct sites for methanation were observed on Ni/TiO_2 and Ni/Al_2O_3. The lowest specific activities were observed for Ni/SiO_2 and $Ni/SiO_2 \cdot Al_2O_3$. For all catalysts, carbon hydrogenation occurred at a lower temperature than carbon monoxide hydrogenation. For both TPR and TPSR, small amounts of ethane were formed and at a lower temperature than methane. The amount of less-active, β-carbon observed in TPSR experiments was very small on all catalysts. These results indicate that at high coverages, carbon hydrogenation does not depend on the support, and thus it is not rate-determining for CO hydrogenation in excess hydrogen. The support is also shown to change the specific rate of carbon monoxide methanation; activity differences seen in steady-state experiments are not just due to differences in site densities.

INTRODUCTION

The rate of carbon hydrogenation was studied on nickel catalysts as a function of support. Since this is one step in the mechanism for CO hydrogenation (*1–9*), which depends significantly on the support (*10–13*), information can be obtained about the reaction mechanism for CO hydrogenation. For example, if carbon hydrogenation is the rate-determining step in methanation, then changing the support should change the rate of carbon hydrogenation since changing the support changes the steady-state methanation rate. Thus, hydrogenation of carbon that was deposited by CO disproportionation was investigated on supported nickel catalysts for four oxide supports, SiO_2, Al_2O_3, TiO_2, and $SiO_2 \cdot Al_2O_3$. The technique of temperature-programmed surface reaction (TPSR) (*4*), in which a catalyst, with a layer of carbon on its surface, is heated at a linear rate in hydrogen, was used. This technique was originally applied to a commercial Ni/Al_2O_3 catalyst (*4*). The various states of carbon observed in that study, however, may not be indicative of those on other catalysts. A recent TPSR study on a high-dispersion Ni/SiO_2 catalyst, for example, observed only one form of carbon (*14*).

For comparison, the specific rates of carbon monoxide hydrogenation were also measured, on the same catalysts, by temperature-programmed reaction (TPR). Many studies have shown that the activity and selectivity depend on the support for CO hydrogenation. Titania-supported nickel has been found to have the highest activity and selectivity to higher hydrocarbons (*10, 11, 15, 16*). However, metal–support interactions can suppress hydrogen chemisorption and thus make calculation of specific activities difficult (*10, 15, 16*). TPR

[1] To whom correspondence should be addressed.

0021-9517/83 $3.00

avoids this problem since it measures specific rates of reaction, independent of surface area measurements. It also has the advantage of determining the number of sites available for reaction. In the present study, Ni/TiO_2 was reduced at 723 K to avoid the occurrence of the SMSI state. To avoid effects of structure sensitivity, nickel catalysts were prepared with low dispersions and similar weight loadings.

Since methane does not readily adsorb on nickel, these experiments are not significantly affected by readsorption (*14*), and thus the peak temperatures are indicative of the specific reaction rates.

EXPERIMENTAL

Temperature-programmed surface reaction (TPSR) and temperature-programmed reaction (TPR) were carried out in atmospheric-pressure hydrogen using an apparatus similar to that described in the literature (*17*). A 100-mg catalyst sample (60–80 mesh) rested on a quartz frit in a tubular quartz reactor (1-cm o.d.). This reactor was heated in an electric furnace which was controlled by a derivative-proportional temperature programmer. A 0.25-mm-o.d. shielded thermocouple was inserted in the catalyst sample to measure temperature and to provide feedback to the temperature programmer.

A typical TPSR experiment was carried out as follows. A passivated nickel catalyst sample was preheated at 773 K (723 K for Ni/TiO_2) in hydrogen for 2 h. The catalyst was then held at the pretreatment temperature in helium for 20 min before cooling to room temperature. Carbon was deposited from CO disproportionation by injecting pulses of 10% CO in He over the catalyst, which was held at elevated temperatures (573 to 719 K) in helium flow. The carbon dioxide that formed was detected by the mass spectrometer and used as an indication of carbon coverage (*1, 3, 4*). The amount of CO that coadsorbed with the carbon was a function of CO exposure, catalyst temperature, and how quickly the catalyst was cooled. Following CO exposure, the catalyst was cooled in helium to 298 K, and the helium carrier was replaced by hydrogen, which had a flow rate of 250 cm^3/min. The catalyst was then heated in hydrogen at 1 K/s to 773 K (723 K for Ni/TiO_2). Immediately downstream from the reactor, the products were continuously sampled through a leak valve and analyzed by a UTI quadrupole mass spectrometer, which was located in a turbomolecular-pumped vacuum chamber.

For TPR experiments, a similar procedure was followed except that the catalyst was exposed to CO at room temperature in hydrogen flow. Repeated injections of CO were used until saturation coverage was obtained.

Catalysts. Nickel catalysts were prepared by wet impregnation of nickel nitrate hydrate using a procedure described in the literature (*18*). The impregnated supports were dried in vacuum at 400 K and then reduced in hydrogen without calcination. During reduction the catalysts were heated at 1.5 K/min to 503 K, held at 503 K for 2 h, and then heated to their final reduction temperature at 1.5 K/min and held there for 12 h. The catalysts were then held at their final reduction temperature in helium for 20 min before being cooled to 298 K and passivated with oxygen in helium. The final reduction temperatures were 773 K for Ni/SiO_2, Ni/Al_2O_3, and $Ni/SiO_2 \cdot Al_2O_3$ and 723 K for Ni/TiO_2 (*10, 11*).

The nickel content of Ni/TiO_2 catalysts was measured by a gravimetric technique. Atomic absorption was used for the other catalysts. Carbon monoxide and hydrogen adsorption was measured by a pulse technique in the TPD apparatus (*19*) and the hydrogen adsorption was used to estimate dispersions. The dispersions were between 0.03 and 0.07. These values are probably lower limits since some catalysts may not be completely reduced and because the pulse technique yields a lower estimate of dispersion. Also, because of metal–support effects, hydrogen adsorption may give

a low estimate of dispersion on Ni/TiO_2. The ratio of CO/H adsorption was larger on Ni/TiO_2 catalysts than on Ni/SiO_2 or $Ni/SiO_2 \cdot Al_2O_3$.

Davison silica (Grade 57) and silica-alumina (Grade 970) were used for the supports. The alumina was Kaiser A-201 and the titania was Degussa P-25.

RESULTS

Carbon Hydrogenation (TPSR)

Carbon was deposited by CO disproportionation. Most of the data are for carbon deposition at 573 K. Some carbon monoxide was coadsorbed with the carbon. During programmed heating in hydrogen, this carbon and carbon monoxide reacted to methane and ethane. Methane formation began near room temperature and was observed over a wide temperature range. Figure 1, which shows methane formation on Ni/Al_2O_3, is typical of the TPSR results on the five supported-nickel catalysts. For Ni/Al_2O_3, a broad methane peak was seen with a peak temperature of 417 K and a smaller shoulder was seen near 500 K. From TPR for CO hydrogenation, this shoulder was found to correspond to CH_4 from hydrogenation of coadsorbed CO. When the CO hydrogenation curve was subtracted from the total curve, the resulting methane curve was from carbon hydrogenation and is shown as the dashed curve in Fig. 1. Methane from carbon hydrogenation on Ni/Al_2O_3 consisted of a broad peak at 417 K and a very small peak near 600 K.

Similar results were seen for the other catalysts though the amount of coadsorbed CO was different. This depended on the support (*20*) and on how long the CO was flushed from the system before cooling. As indicated in Fig. 2, 20% of the total methane from Ni/SiO_2 was from CO hydrogenation. The high-temperature peak in this figure corresponds exactly to CO methanation on Ni/SiO_2 (*21*). No methane was observed above 550 K on Ni/SiO_2. A small amount of ethane was observed at low temperatures, as shown in Fig. 2.

On the other three catalysts, less than 10% of the CH_4 was from coadsorbed CO. A very small amount of CH_4 from coadsorbed CO was observed on Ni/TiO_2; Fig. 3 shows the TPSR spectra for 5% Ni/TiO_2. As on Ni/SiO_2, ethane had a lower peak temperature (382 K) than methane (418 K). The amount of ethane formed was small (0.3 μmol/g) relative to methane (13 μmol/g).

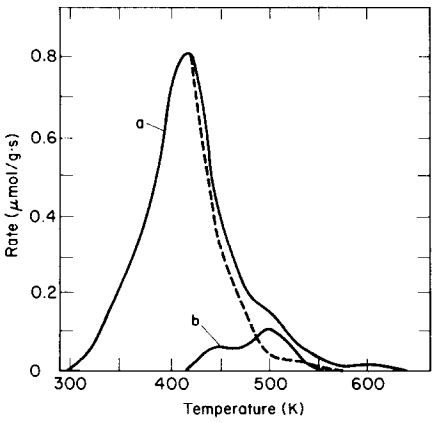

FIG. 1. Methane from 10.5% Ni/Al_2O_3 catalyst. (a) Carbon monoxide exposure at 573 K. (b) Contribution from carbon monoxide hydrogenation. The dashed curve corresponds to the difference of curves a and b.

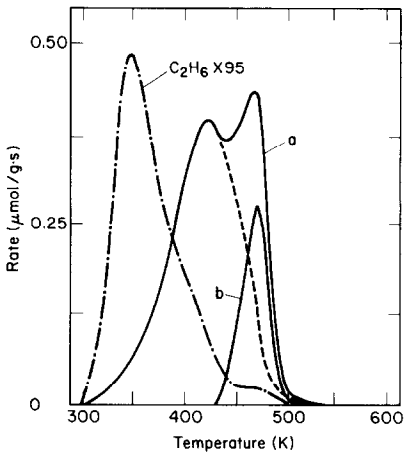

FIG. 2. 16% Ni/SiO_2 catalyst. Methane from (a) carbon monoxide exposure at 573 K. (b) Contribution from carbon monoxide hydrogenation. The dashed curve corresponds to the difference of curves a and b. (c) Ethane from carbon monoxide exposure at 573 K.

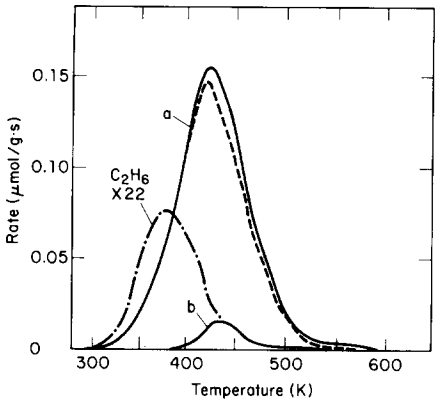

FIG. 3. 5% Ni/TiO_2 catalyst. Methane from (a) carbon monoxide exposure at 573 K. (b) Contribution from carbon monoxide hydrogenation. The dashed curve corresponds to the difference of curves a and b. (c) Ethane from carbon monoxide exposure at 573 K.

The methane peak temperatures for carbon hydrogenation were between 413 and 423 K for the five catalysts. The halfwidths ranged from 76 to 82 K and the three-quarter widths from 47 to 53 K. These values are for the dashed curves in the figures; the contribution from CO hydrogenation was subtracted out using the TPR data for CO hydrogenation.

Because the peak temperatures and widths are similar on all five catalysts, the activation energies calculated from these measurements are very similar. A first-order process was assumed since the methane peak temperatures did not vary with the amount of deposited carbon, which was varied by changing the number of CO pulses. McCarty and Wise (*4*) also observed this on their Ni/Al_2O_3 catalyst. Table 1 lists the activation energies calculated for a first-order process, using both the halfwidth and three-quarter width equations (*22*). Excellent agreement is obtained for these two equations. Preexponential factors calculated from Redhead's formula (*23*) ranged from 3×10^3 to 9×10^3 s^{-1}, and these were used to calculate the rate constants at 550 K that are listed in Table 1. The rate constants vary only by a factor of 1.7; within experimental error, the rate of carbon hydrogenation is the same on these catalysts.

For 5% Ni/TiO_2 the temperature of CO exposure was varied over a wider range. At 460 K, no CO_2 formed from CO exposure and the resulting CH_4 was similar in peak temperature and width to that obtained for TPR. That is, no carbon was formed at 460 K. Carbon monoxide exposure at 623 K resulted in a CH_4 peak similar to that for 573 K exposure but an additional low-temperature shoulder appeared and a small amount of less-reactive carbon, as indicated by a peak at 660 K, was seen. The peak amplitude of this peak was only 4% of the 417 K peak. As the exposure temperature increased to 720 K, the width of the peak at 417 K increased and an additional small peak was seen at 550 K.

Carbon Monoxide Hydrogenation (TPR)

Carbon monoxide which was adsorbed at room temperature reacted to methane, water, and higher hydrocarbons. Unreacted CO also desorbed at low temperatures. The support significantly influenced the rate of

TABLE 1

Methane Activation Energies and Rate Constants: Carbon Hydrogenation

Catalyst	Activation energy (kJ/mol)		Rate constant at 550 K (s^{-1})
	½-width method	¾-width method	
16% Ni/SiO_2	40	40	0.37
9.7% $Ni/SiO_2 \cdot Al_2O_3$	42	40	0.45
10.5% Ni/Al_2O_3	41	44	0.50
9.9% Ni/TiO_2	40	40	0.50
5% Ni/TiO_2	43	44	0.58
10% Ni/SiO_2 (Ref. *27*)	38		—
2% Ni/SiO_2 (Ref. *27*)	62		—
25% Ni/Al_2O_3 (Ref. *4*)	71		0.5

hydrocarbon formation and the number of sites available for CO hydrogenation.

A single methane peak was seen on the Ni/SiO_2 catalyst, as reported previously for a 6.9% Ni/SiO_2 (*21*). On $Ni/SiO_2 \cdot Al_2O_3$, a somewhat broader peak at lower temperature was observed. In contrast, a very narrow CH_4 peak at a significantly lower temperature was observed for both Ni/TiO_2 catalysts. As shown in Fig. 4, a second, small methane peak was also seen on both Ni/TiO_2 catalysts. On Ni/Al_2O_3, two distinct peaks of similar amplitudes were observed (see Fig. 5).

The peak temperatures and curve widths are summarized in Table 2. A lower peak temperature is indicative of a higher specific rate. Thus, the specific activity for CO hydrogenation is in the order

$$5\%\ Ni/TiO_2 \geq 9.9\%\ Ni/TiO_2 > Ni/Al_2O_3 > Ni/SiO_2 \cdot Al_2O_3 > Ni/SiO_2$$

Some sites, or some forms of adsorbed CO, on Ni/Al_2O_3 and Ni/TiO_2 have lower specific activities.

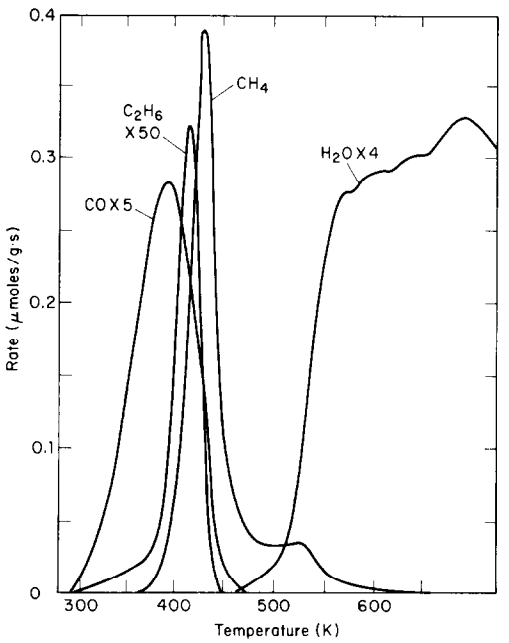

FIG. 4. TPR product spectra for CO adsorption on 5% Ni/TiO_2 at 300 K.

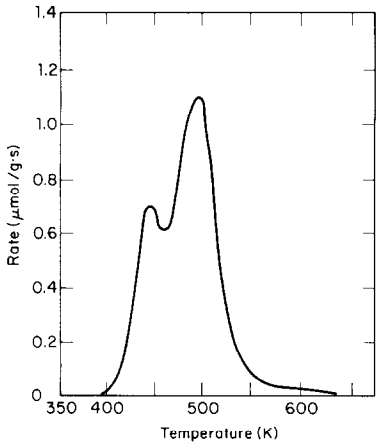

FIG. 5. TPR spectra for methane from CO adsorbed at 300 K on 10% Ni/Al_2O_3.

Estimates of activation energies can be made from the peak temperatures and halfwidths (or three-quarter widths) (*22*). These are only estimates but they are useful for comparing catalytic activities. Shape factors (*24*) were close to first-order values for Ni/SiO_2 and Ni/TiO_2; for $Ni/SiO_2 \cdot Al_2O_3$ the shape factor was larger than expected for first order. Because of the overlapping peaks, shape factors could not be measured for Ni/Al_2O_3. Except for $Ni/SiO_2 \cdot Al_2O_3$, skewness parameters (*22*) were close to

TABLE 2

Methane Peak Temperature and Peak Widths: CO Hydrogenation

Catalyst	Peak temperature (K)	½-Width (K)	¾-Width (K)
16% Ni/SiO_2	484	44	26
9.7% $Ni/SiO_2 \cdot Al_2O_3$	471	59	34
10.5% Ni/Al_2O_3	445	36[a]	25[a]
	495	56[a]	32
9.9% Ni/TiO_2	438	27	17
	506	—	—
5% Ni/TiO_2	434	28	16
	525	—	—

[a] Approximate widths; peak overlap prevented accurate determination.

first-order processes though somewhat more negative (−16 to −23 for halfwidths and −10 to −12.5 for three-quarter widths). For $Ni/SiO_2 \cdot Al_2O_3$ the skewness parameters were significantly outside the first-order range. Also, as expected for a first-order process, on Ni/SiO_2 the peak temperature did not vary with initial coverage (*21*). Thus, a first-order process was assumed in calculating activation energies. Preexponential factors were estimated from Redhead's formula (*23*).

Activation energies from the half and three-quarter widths (*22*) were in good agreement though the energies for the narrower peaks were very sensitive to accuracy of the measurements. Reasonable values of activation energies and preexponential factors were obtained (see Table 3).

Rate constants at 500 and 550 K, calculated from these kinetic parameters, showed activities in the same order determined from the peak temperatures except for $Ni/SiO_2 \cdot Al_2O_3$ (see Table 4). The Ni/TiO_2 catalysts were significantly more active than Ni/SiO_2 and they had the highest activation energies. The mean rate constant for Ni/Al_2O_3 is equal to the sum of the rate constants for the two peaks, multiplied by the fraction of methane in each peak.

Ethane was detected in small quantities (less than 1% of the methane quantity) because of the large hydrogen excess. On some catalysts propane and butane were observed, but in even smaller amounts. For all catalysts, ethane formation began near room temperature and the ethane peak temperature was lower than that of methane. The ethane peaks were rather broad on silica- and silica-alumina-supported nickel but a very narrow ethane peak was observed on each Ni/TiO_2 catalyst (see Fig. 4). On Ni/Al_2O_3, multiple peak ethane spectra, with very small quantities of ethane, were seen. The specific activities for ethane was in the same order as for methane (see Table 5).

Water and unreacted carbon monoxide

TABLE 3

Methane Kinetic Parameters: CO Hydrogenation

Catalyst	Activation energies (kJ/mol)		Preexponential factor (s^{-1}) (based on ½-width)
	½-Width method	¾-Width method	
16% Ni/SiO_2	103	111	7×10^9
9.7% $Ni/SiO_2 \cdot Al_2O_3$	73	80	3×10^6
10.5% Ni/Al_2O_3			
T_p = 445 K	107[a]	97[a]	2×10^{11}
T_p = 495 K	83[a]	94	2×10^7
9.9% Ni/TiO_2	139	140	3×10^{15}
5% Ni/TiO_2	132	147	6×10^{14}

[a] Approximate values; peak overlap prevented accurate determination.

TABLE 4

Methane Rate Constants: CO Hydrogenation

Catalyst	Rate constant k (s^{-1})	
	500 K	550 K
16% Ni/SiO_2	0.12	1.1
9.7% $Ni/SiO_2 \cdot Al_2O_3$	0.11	0.49
10.5% Ni/Al_2O_3		
T_p = 445 K	1.3	13
T_p = 495 K	0.04	0.25
Mean value	0.42	4.0
9.9% Ni/TiO_2	9.0	170
5% Ni/TiO_2	9.7	160

TABLE 5

Ethane Peak Temperatures and Halfwidths: CO Hydrogenation

Catalyst	Peak temperature (K)	Halfwidths (K)
16% Ni/SiO_2	461	66
9.7% $Ni/SiO_2 \cdot Al_2O_3$	443	81
10.5% Ni/Al_2O_3	370	—
	431	43
	483	—
9.9% Ni/TiO_2	425	30
5% Ni/TiO_2	422	27

were also observed. As reported previously (*21*), on Ni/SiO_2 water formed at the same temperature as methane. On $Ni/SiO_2 \cdot Al_2O_3$, water was delayed to 514 K, and on Ni/Al_2O_3 and Ni/TiO_2, readsorption on the support delayed water to high temperature (*25*), as shown in Fig. 4. Unreacted carbon monoxide desorbed, starting at room temperature, with a peak temperature lower than methane. Figure 4 shows CO from Ni/TiO_2.

One experiment was carried out in which additional carbon monoxide was coadsorbed with deposited carbon. Carbon monoxide was exposed to the 5% Ni/TiO_2 catalyst at 573 K, the catalyst was cooled to 298 K, and additional CO exposure was given. The resulting methane curve was a linear combination of CH_4 from adsorbed CO and CH_4 from carbon.

DISCUSSION

The rate of CO hydrogenation at 550 K varies by two orders of magnitude for TPR hydrogenation on these catalysts. Since the dispersions and weight loadings are similar, the differences are apparently due to metal–support interactions. Steady-state kinetic experiments have shown that these supports can significantly change catalyst activity and selectivity (*10, 11, 15*). However, carbon, which is an intermediate in CO hydrogenation on nickel (*1–9*), has a rate of hydrogenation which varies in TPSR only by a factor of 1.7, which is within experimental error. The activation energy for carbon hydrogenation is also independent of support, and it is significantly lower than the values of 90 to 138 kJ/mol measured for steady-state CO hydrogenation (*10–12, 15, 26*) and from TPR. Thus, carbon hydrogenation does not appear to be the rate-determining step in CO hydrogenation in excess hydrogen.

It is important to emphasize that the carbon hydrogenation results are for a transient measurement and care must be taken in extending them to steady-state conditions. Carbon monoxide hydrogenation by TPR appears to be consistent with steady-state data. However, the results for carbon hydrogenation were obtained for saturation coverage while carbon coverage is significantly lower than this at steady-state conditions.

Carbon Hydrogenation

McCarty and Wise (*4*) observed that carbon which they labeled α-carbon was hydrogenated to methane on Ni/Al_2O_3 at a lower temperature than adsorbed carbon monoxide. They concluded that α-carbon was hydrogenated at a sufficiently fast rate to make it a likely intermediate in methanation. Another TPSR study on a Ni/SiO_2 catalyst observed the same thing (*14*). Similarly, Rabo *et al.* (*3*) observed in pulse reaction experiments that surface carbon was more reactive then chemisorbed, but nondissociated CO. They (*3*) found that at room temperature some carbon reacted to form C_1–C_4 hydrocarbons, while adsorbed CO was inert to hydrogen at room temperature. Thus, the present study of carbon hydrogenation for nickel on various supports is in agreement with these previous studies.

During TPSR, carbon is hydrogenated at a lower temperature than CO and thus at the peak temperature (approximately 420 K), the rate of carbon hydrogenation is higher than that of CO hydrogenation. This may not be true at higher temperatures since carbon hydrogenation has a significantly lower activation energy than CO hydrogenation. Thus, comparison of TPSR rate constants at 550 K (see Table 1) with those for CO hydrogenation in TPR (Table 4) indicate that the rate constants are close to each other for Ni/SiO_2 and $Ni/SiO_2 \cdot Al_2O_3$. For Ni/TiO_2 catalysts, however, the rate constants for CO hydrogenation are significantly larger than those for carbon hydrogenation. For steady-state hydrogenation, the relative surface coverages of carbon and carbon monoxide determine which reaction is faster. The differences in relative rates of CO and carbon hydrogenation for Ni/SiO_2 and Ni/TiO_2 may be related

to the significant differences in selectivities observed during steady-state reaction.

Galuszka *et al.* (*8*) reported that at 373 K the rates of CO dissociation and carbon hydrogenation on Ni/Al_2O_3 were comparable and the rate-determining step could shift depending on the pressures of H_2 and CO. Rabo *et al.* (*3*) had earlier also pointed out that no data was available which would prove unequivocably the superior reactivity of surface carbon over chemisorbed CO at the higher temperatures which are more relevant to hydrocarbon synthesis.

The average value of activation energy for carbon hydrogenation on the five nickel catalysts is 42 kJ/mol. On a 10% Ni/SiO_2 catalyst, Van Ho and Harriot (*27*) measured activation energies from initial rate data at different temperatures; carbon was deposited by CO disproportionation by 573–623 K. They reported a similar activation energy of 38 kJ/ml. They, however, reported that activation energy depended on dispersion and they observed $E = 62$ kJ/mol for a higher dispersion, 2% Ni/SiO_2 catalyst. Applying halfwidth analysis to CH_4 from carbon hydrogenation on a high-dispersion Ni/SiO_2 catalyst studied by TPSR (*14*) gives a similar activation energy of 63 kJ/mol. McCarty and Wise (*4*) used TPSR and heating rate variation to measure an activation energy of 71 kJ/mol for a low-dispersion, commercial Ni/Al_2O_3 catalyst. Our activation energy is significantly lower than this but our preexponential factor is also almost three orders of magnitude lower, so the specific rate of reaction is very similar in both studies (see Table 1). Galuszka *et al.* (*8*) measured an even higher activation energy of 84 ± 17 kJ/mol for carbon hydrogenation on Ni/Al_2O_3.

McCarty and Wise (*4*) also observed, with TPSR, a significant amount of less-reactive carbon. They labeled a methane peak at 650 K as β-carbon and indicated it was formed by deactivation of α-carbon (peak at 420 K) (*28*). Near monolayer coverages, the ratio of β-carbon to α-carbon was 0.5, but a higher ratio was observed at higher carbon coverage and at higher carbon deposition temperatures (*4*). We observed a much smaller amount of β-carbon. The ratio of β- to α-carbon was 0.04 on Ni/TiO_2 and Ni/Al_2O_3, and no β-carbon was detected on $Ni/SiO_2 \cdot Al_2O_3$ or Ni/SiO_2. Similarly, no β-carbon was seen on a higher dispersion Ni/SiO_2 (*14*). Higher deposition temperatures did not significantly increase the β-carbon on Ni/TiO_2. These differences from McCarty and Wise's results may be caused by the added ingredients in their catalyst. They stated (*4*) that the local crystal structure of the nickel governs the type of carbon formed.

The other significant difference from the previous TPSR study (*14*) was that we observed carbon monoxide coadsorbed with carbon. However, a large amount of coadsorbed CO was only seen on Ni/SiO_2 and very little was seen on Ni/Al_2O_3. Carbon monoxide desorption depends on the support (*20*). This peak near 470 K was from carbon monoxide and was not due to a less-active carbon. This was verified by monitoring the water signal during TPSR. No water was observed while CH_4 formed at 423 K on Ni/SiO_2, but a significant water peak was seen at 470 K, indicating that CO was being hydrogenated to CH_4 and H_2O. When additional carbon monoxide was coadsorbed, at 298 K, with carbon on 5% Ni/TiO_2, the presence of a large amount of coadsorbed CO did not appear to significantly affect the rate of carbon hydrogenation since the resulting spectrum was a linear combination of carbon and carbon monoxide dehydrogenation. During steady-state methanation, both C and CO are present on the surface.

During TPSR, very small amounts of carbon were hydrogenated to ethane, which formed at a lower temperature than methane. This ethane, which was only observed on Ni/TiO_2 and Ni/SiO_2, was at lower temperatures than ethane from hydrogenation of chemisorbed CO in TPR. On Ni/TiO_2, the ethane peak temperature for carbon hydrogenation was 40 K lower than ethane

from hydrogenation of chemisorbed CO. Thus, carbon hydrogenates to both ethane and methane at lower temperatures than CO does. Rabo *et al.* (*3*) observed that when hydrogen was pulsed over deposited carbon, hydrocarbons up to C_4 were seen and higher temperatures favored methane over the higher hydrocarbons.

CO Hydrogenation

As seen in steady-state experiments, the support has a significant effect on catalytic activity (*10, 11, 15, 16*). The TPR experiments show that specific activities change with the support; the changes are not due to difficulties in measuring surface areas. The activation energies for methane, as measured from halfwidths, also change with support, and in all cases are larger than the activation energies for carbon hydrogenation.

The order of activities, with Ni/TiO_2 being the most active, are in general agreement with the literature, which has reported Ni/TiO_2 catalysts are one to two orders of magnitude more active than Ni/SiO_2 (*10, 11*). The Ni/Al_2O_3 is more active than Ni/SiO_2 and this has been observed on a number of other Group VIII metals by Fujimoto *et al.* (*29*). Also, higher activation energies for Ni/TiO_2 have been seen in steady-state experiments (*15, 16*).

The support can also cause the occurrence of multiple reaction sites, with different activities, and on Ni/Al_2O_3 and Ni/TiO_2, two distinct methane peaks were seen. The activities of multiple sites are averaged in steady-state experiments, but separated by TPR. Two overlapping methane peaks may also be present on $Ni/SiO_2 \cdot Al_2O_3$ since the methane curves were broad, the skewness factors and shape factors were outside the first-order range and the activation energies were somewhat low.

The peak temperatures, curve shapes, and the amount of ethane formed also changed with the support. The ethane peak temperature in each case was lower than that for the methane peak. The amount of ethane was small because of the large $H_2:CO$ ratio.

CONCLUSIONS

Temperature-programmed reaction (TPR) and surface reaction (TPSR) show that the activation energy of carbon hydrogenation on nickel at high carbon coverage is independent of support (SiO_2, TiO_2, Al_2O_3, $SiO_2 \cdot Al_2O_3$) and equal to 42 kJ/mol. In contrast, the activation energy of CO hydrogenation varies between 72 and 139 kJ/mol. Thus at low temperatures, carbon hydrogenation does not appear to be the rate-determining step for CO hydrogenation on nickel. However, these experiments are for high carbon coverages, and steady-state conditions may correspond to significantly lower carbon coverage.

These studies also demonstrate the ability of TPR to measure specific catalytic activities, independent of surface area measurements. The order of specific activity for CO hydrogenation to methane at 550 K is

$$Ni/TiO_2 > Ni/Al_2O_3 > Ni/SiO_2 > Ni/SiO_2 \cdot Al_2O_3.$$

On Ni/Al_2O_3 and Ni/TiO_2, less active sites are also present.

Both carbon and CO were found to hydrogenate to ethane at a lower temperature than methane and very little inactive β-carbon formed on the nickel catalysts.

ACKNOWLEDGMENTS

We gratefully acknowledge support of this work by the Mobil Foundation and the University of Colorado Council for Research and Creative Work. We also thank the National Science Foundation for Equipment Grant CPE-7923208. We would like to thank Isabelle Corfa and Kevin M. Larson for experimental assistance.

REFERENCES

1. Wentrcek, P. R., Wood, B. J., and Wise, H., *J. Catal.* **43,** 363 (1976).
2. Arai, M., and Ponec, V., *J. Catal.* **44,** 439 (1976).
3. Rabo, J. A., Risch, A. P., and Poutsma, M. L., *J. Catal.* **53,** 295 (1978).

4. McCarty, J. G., and Wise, H., *J. Catal.* **57,** 406 (1979).
5. Biloen, P., Helle, J. N., and Sachtler, W. M. H., *J. Catal.* **58,** 95 (1979).
6. Goodman, D. V., Kelley, R. D., Madey, T. E., and Yates, J. T., *J. Catal.* **64,** 226 (1980).
7. Ponec, V., *Catal. Rev. Sci. Eng.* **18,** 151 (1978).
8. Galuszka, J., Chang, J. R., and Amenomiya, Y., Proceedings of 7th International Congress on Catalysis, Tokyo, June, 1980, p. 529.
9. Bell, A. T., *Catal. Rev. Sci. Eng.* **23,** 203 (1981).
10. Vannice, M. A., and Garten, R. L., *J. Catal.* **56,** 236 (1979).
11. Bartholomew, C. H., Pannell, R. B., and Butler, J. L., *J. Catal.* **65,** 335 (1980).
12. Vannice, M. A., *J. Catal.* **44,** 152 (1976).
13. Smith, J. S., Thrower, P. A., and Vannice, M. A., *J. Catal.* **68,** 270 (1981).
14. Zagli, E., and Falconer, J. L., *Appl. Catal.* **4,** 135 (1982).
15. Vannice, M. A., *J. Catal.* **66,** 242 (1980).
16. Vannice, M. A., *J. Catal.* **74,** 199 (1982).
17. Zagli, A. E., Falconer, J. L., and Keenan, C. A., *J. Catal.* **56,** 453 (1979).
18. Bartholomew, C. H., and Farrouto, R. J., *J. Catal.* **45,** 41 (1976).
19. Freel, J., *J. Catal.* **61,** 7 (1980).
20. Ozdogan, S. Z., Master's Thesis, University of Colorado, 1982.
21. Falconer, J. L., and Zagli, A. E., *J. Catal.* **62,** 280 (1980).
22. Chan, C. M., Aris, R., and Weinberg, W. H., *Appl. Surf. Science* **1,** 360 (1978).
23. Redhead, P. A., *Vacuum* **12,** 203 (1962).
24. Ibok, E. E., and Ollis, D. F., *J. Catal.* **66,** 391 (1980).
25. Kester, K. B., Zagli, A. E., and Falconer, J. L., in preparation.
26. Vannice, M. A., *J. Catal.* **50,** 228 (1977).
27. Van Ho, S., and Harriot, P., *J. Catal.* **66,** 272 (1980).
28. McCarty, J. G., Wentrcek, P. R., and Wise, H., presented at National ACS Meeting, Chicago, Illinois, 1977.
29. Fujimoto, K., Kameyama, M., and Kunugi, T., *J. Catal.* **61,** 7 (1980).